J. Fluid Mech. (1998), *vol.* 361, *pp.* 275–296. Printed in the United Kingdom

Withdrawal from a two-layer inviscid fluid in a duct

By LAWRENCE K. FORBES[1] AND GRAEME C. HOCKING[2]

[1]Department of Mathematics, University of Queensland, St. Lucia, Queensland, 4072, Australia

[2]Department of Mathematics and Statistics, Murdoch University, Murdoch, Western Australia, 6150, Australia

(Received 25 July 1996 and in revised form 16 December 1997)

The steady simultaneous withdrawal of two inviscid fluids of different densities in a duct of finite height is considered. The flow is two-dimensional, and the fluids are removed by means of a line sink at some arbitrary position within the duct. It is assumed that the interface between the two fluids is drawn into the sink, and that the flow is uniform far upstream. A numerical method based on an integral equation formulation yields accurate solutions to the problem, and it is shown that under normal operating conditions, there is a solution for each value of the upstream interface height. Numerical solutions suggest that limiting configurations exist, in which the interface is drawn vertically into the sink. The appropriate hydraulic Froude number is derived for this situation, and it is shown that a continuum of solutions exists that are supercritical with respect to this Froude number. An isolated branch of subcritical solutions is also presented.

1. Introduction

In reservoirs, cooling ponds or solar ponds, the fluid very often does not occur as a homogeneous entity, but rather stratifies into two or more layers of different density. Reservoirs, in particular, may possess a layer of fresh water overlying a deeper layer into which salts or various pollutants may have entered.

It is often vital to the management of these reservoirs or ponds to know at what rate fluid can be withdrawn from one layer, without entraining fluid from the neighbouring layer. In a reservoir, for example, it may be necessary to remove a lower layer of polluted water, to prevent the entire reservoir from becoming contaminated in the event of a large-scale disruption that mixes up the two layers. It is therefore important to know the conditions under which the lower fluid can be withdrawn, in a manner which does not involve the fresh upper layer.

Recent research has shown that there may be (at least) three different types of flow involving the withdrawal of a lower fluid in a two-layer system. In the first type of flow, only the lower fluid is withdrawn and the interface between the fluids rises to form a stagnation point directly above the sink. A second single-layer flow type also exists, which possesses an interface that is pulled down sharply to form a cusp above the sink, but does not enter it directly. In the third flow type, the interface is pulled right into the sink, so that both fluids are withdrawn.

The present paper is concerned with this third solution type, in which both fluids are withdrawn simultaneously. We consider a two-dimensional system in which both

fluids are of finite depth; the flow therefore occurs in a duct, with a rigid plane below the fluids and a rigid surface above. The two layers are separated by a sharp interface. Withdrawal is envisaged to occur through a mathematical line sink at some arbitrary height within the duct, and the interface is drawn right into this singular withdrawal point. For simplicity, both fluids are assumed to be inviscid and to flow irrotationally.

There has been a great deal of recent work on these withdrawal problems, both as a result of their importance to reservoir management as well as their intriguing scientific interest, since many basic questions concerning these deceptively simple flow problems remain unanswered. Solutions of the first type, in which the interfacial free surface rises to form a stagnation point, appear to have been discussed first by Peregrine (1972). He suggested that a limiting flow would eventually be achieved, for sufficiently high withdrawal rate, at which the interface would form a secondary stagnation point enclosing a 120° corner, exactly as for the classical gravity waves of Stokes. For *three-dimensional* axisymmetric flows into a point sink in infinitely deep fluid, this is evidently what occurs, as the work of Forbes & Hocking (1990) shows, but for two-dimensional flows into a line sink the situation is much less clear. Hocking & Forbes (1991) re-examined the Peregrine solution in infinitely deep fluid, and found that some sort of limiting flow appeared to exist at a Froude number (dimensionless withdrawal rate) of about 1.4, but that no obvious physical mechanism, such as a breaking wave at the interface, presented itself as an explanation for this behaviour. In a later paper in which the effects of surface tension were included, Forbes & Hocking (1993) presented some evidence to suggest that the limiting behaviour may be associated with a mathematical singularity related to a fold bifurcation.

These solutions of the first type described above, having a stagnation point on the interface directly above the sink, also exist in finite-depth flows in two-dimensions. (The corresponding solutions for three-dimensional axisymmetric flow have been presented recently by Forbes, Hocking & Chandler (1996), but these flows are not discussed further here.) Mekias & Vanden-Broeck (1989) computed supercritical solutions, for which the Froude number based on fluid depth is greater than 1, using a numerical scheme based on a series expansion. These flows have a uniform stream at infinity, with the free surface rising to form a stagnation point above the sink. The corresponding solutions for *subcritical* flow (for which the depth-based Froude number is less than 1) were computed by Hocking & Forbes (1992), using both a Nekrasov formulation of the problem, as well as a direct integral equation approach. These authors again obtained solutions with a uniform (subcritical) flow at infinity and a stagnation point on the interface above the sink. The solutions were found to break down at some limiting value of the Froude number, for reasons that were again not clear. In an independent study, Mekias & Vanden-Broeck (1991) also solved this subcritical withdrawal problem in finite depth, but unlike Hocking & Forbes (1992) who concluded that waves far from the line sink would not occur, these authors obtained a regular wave train downstream.

Solutions of the second type, in which the interface is drawn down to form a cusp above the sink, are likewise not fully understood, although they have been in the literature for a long time. They were first reported by Sautreaux (1901), and more solutions of this type were obtained by Craya (1949). In fluid of infinite depth, Tuck & Vanden-Broeck (1984) showed numerically that such flows only exist at one value of the Froude number (withdrawal rate), and so their relationship to other types of flow remains unclear. It has been speculated that these solutions represent the transition to flows of the third type described above, in which the interface falls right into the sink

and both fluids are then withdrawn. If this is the case, then these flows are clearly of importance to the management of reservoirs. This speculation has been examined further experimentally by Hocking (1991) and Wood & Lai (1972), for example. In finite-depth fluids, these cusped solutions also exist, and have been computed in detail by Hocking (1985) and Vanden-Broeck & Keller (1987). In that case, such solutions may exist for all Froude numbers, and Hocking (1988) and Vanden-Broeck & Keller (1987) even obtained a closed-form solution of this type valid for infinite Froude number.

Solutions for flow of the third type, in which both layers are withdrawn simultaneously and the interface itself enters the sink, have been computed only recently by Hocking (1995). He considered the case when both fluids are of infinite depth, so that the overall fluid region is of unbounded extent, and gave strong numerical evidence to suggest that the cusped solutions of the second type, discussed above, do indeed correspond to a transition to a flow with both layers entrained into the sink. This important result justifies interest in these types of flow, from the practical standpoint of reservoir operation and management. (For *three-dimensional* axisymmetric Stokes flow of viscous fluids, Lister (1989) has computed some steady solutions with the interface passing into the sink. In that case, the results were primarily of geothermal interest.)

The present paper aims to extend Hocking's (1995) work, by studying in detail the case when both fluids are of finite depth, and the interface between them is drawn into the sink. For simplicity, it is assumed that the fluids are bounded above and below by horizontal planes, so that the only free surface is the interface between the fluids, which is drawn into the line sink. The combination Froude number appropriate to this situation is derived in the Appendix, and it is shown that both subcritical and supercritical solutions exist. In the supercritical case, there is a continuum of solutions in which the height of the interface far upstream is free to be specified for a given Froude number, but in the subcritical case, the solutions exist only as an isolated branch, with an interface height that is determined as part of the solution.

2. Formulation of the two-layer withdrawal problem

In two-dimensional steady flow, consider a horizontal duct of total height L, containing two fluids. The upper fluid (referred to here as fluid 1) is of density ρ_1 and the heavier lower fluid (fluid 2) has density ρ_2 ($\rho_2 > \rho_1$). Suppose there is a line sink within the duct, at some height S_2 above the lower surface of the duct. The sink withdraws both fluids simultaneously, at a total volume rate $2Q_T$. A Cartesian coordinate system is placed on the flow, with the x-axis pointing horizontally along the lower surface of the duct and the y-axis pointing vertically. Thus, the line sink is located at the point $(x, y) = (0, S_2)$. The two fluids are assumed to be separated by a sharp interface (of zero thickness), and this interface enters the line sink at some angle α to the horizontal, as shown in figure 1. The downward acceleration of gravity is g.

Far from the sink, the interface is flat, and lies at a height H_2 above the bottom surface of the duct. The upper fluid 1 is therefore of some constant depth H_1 far upstream, with $H_1 + H_2 = L$ (the total depth of the duct). Suppose that, far from the sink, lower layer 2 has some uniform speed c_2 and that the speed in the upper layer is c_1. In addition, suppose that the line sink withdraws upper fluid 1 at the volume flow rate $2Q_1$ and the lower fluid 2 at the rate $2Q_2$. Then it follows that the total

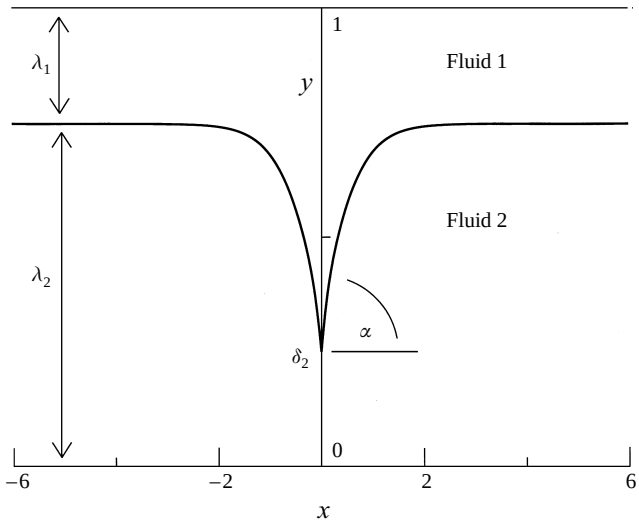

FIGURE 1. An illustrative sketch of the two-layer dimensionless withdrawal problem. (The interface is taken from an actual solution, obtained with $\delta_2 = 0.25$, $D = 0.9$, $F_T = 0.2$.)

withdrawal rate of fluid is $2Q_T = 2Q_1 + 2Q_2$ and by conservation of mass in each fluid layer

$$Q_1 = c_1 H_1 \quad \text{and} \quad Q_2 = c_2 H_2. \tag{2.1}$$

At this point it is desirable to introduce dimensionless coordinates and variables. This may be done in a number of different ways, but since the total duct depth L and the total withdrawal rate $2Q_T$ would be readily measurable quantities in an experiment, it seems most natural to use them as the basic units of length and volume flow rate. Therefore, all lengths are referenced to L, and speeds to the quantity Q_T/L.

In these new dimensionless variables, there are eight non-dimensional parameter groupings. These are the dimensionless sink elevation parameter $\delta_2 = S_2/L$, and the depths of the two fluid layers $\lambda_1 = H_1/L$ and $\lambda_2 = H_2/L$ far upstream of the sink. These two depths are clearly related through the equation $\lambda_1 + \lambda_2 = 1$, as is illustrated in figure 1. In addition, there is a non-dimensional density ratio $D = \rho_1/\rho_2$, and it is necessary to impose the restriction $D < 1$ to obtain physically meaningful solutions. The relative volume fractions withdrawn from layers 1 and 2 are $\theta_1 = Q_1/Q_T$ and $\theta_2 = Q_2/Q_T$, and these are related by means of the equation $\theta_1 + \theta_2 = 1$. The angle α at which the interface enters the sink is also of importance, and is illustrated in figure 1. Finally, there is the total Froude number $F_T = Q_T/(gL^3)^{1/2}$ which measures the volume rate at which the two fluids are removed from the duct.

Of these eight dimensionless parameters, it will be seen that, in the cases of most interest, only four of these are truly independent. Clearly two of the parameters could be removed at once, if desired, by means of the trivial relations

$$\lambda_1 + \lambda_2 = 1 \quad \text{and} \quad \theta_1 + \theta_2 = 1. \tag{2.2}$$

An analysis of the flow near the line sink gives another relationship between these parameters, as will be seen presently (equation (2.13)), and one more parameter must be determined as part of the solution; this parameter is usually the angle of entry α of the interface into the sink.

The flow speeds c_1 and c_2 in the two fluid layers are measured in these dimensionless

variables by means of two additional Froude numbers F_1 and F_2 in layers 1 and 2 respectively. In the upper fluid, the Froude number far upstream is $F_1 = c_1/(gH_1)^{1/2}$, and the corresponding quantity in the lower fluid is $F_2 = c_2/(gH_2)^{1/2}$. Although it is not strictly necessary to introduce these additional parameters, they may give an indication of relative flow conditions in the two layers. They may be eliminated, if desired, in terms of the eight basic flow parameters defined above, since the conservation of mass conditions (2.1) yield

$$F_1 = \frac{\theta_1 F_T}{\lambda_1^{3/2}} \quad \text{and} \quad F_2 = \frac{\theta_2 F_T}{\lambda_2^{3/2}}. \tag{2.3}$$

These two Froude numbers can also be related to the total Froude number F_T by means of the expression

$$F_T = F_1 \lambda_1^{3/2} + F_2 \lambda_2^{3/2}. \tag{2.4}$$

Since each fluid is assumed to be incompressible and to flow irrotationally, the horizontal and vertical velocity components u_j and v_j in each layer, $j = 1, 2$, can be expressed in terms of velocity potentials ϕ_j and streamfunctions ψ_j according to the usual definitions

$$u_j = \frac{\partial \phi_j}{\partial x} = \frac{\partial \psi_j}{\partial y} \quad v_j = \frac{\partial \phi_j}{\partial y} = -\frac{\partial \psi_j}{\partial x}, \quad j = 1, 2. \tag{2.5}$$

These expressions (2.5) are the Cauchy–Riemann equations of complex variable theory, and they reveal that complex potentials $f_j(z) = \phi_j + \mathrm{i}\psi_j$ may be defined in each layer, $j = 1, 2$, which are analytic functions of the complex coordinate $z = x + \mathrm{i}y$. The velocities may then be written $u_j - \mathrm{i}v_j = \mathrm{d}f_j/\mathrm{d}z$ in each fluid. Far upstream the flow becomes uniform, so that

$$u_j \to -\frac{\theta_j}{\lambda_j} \quad v_j \to 0 \quad \text{as} \quad x \to \infty, \quad j = 1, 2. \tag{2.6}$$

As both the top and bottom surfaces of the duct are assumed to be impermeable, the boundary conditions on these planes then become

$$v_1 = 0 \quad \text{on} \quad y = 1, \quad v_2 = 0 \quad \text{on} \quad y = 0. \tag{2.7}$$

Very close to the sink, the complex potentials in each layer are dominated by the singular behaviour

$$\left.\begin{aligned} f_1 &\to -\frac{2\theta_1}{\pi - 2\alpha} \ln(z - \mathrm{i}\delta_2) \\ f_2 &\to -\frac{2\theta_2}{\pi + 2\alpha} \ln(z - \mathrm{i}\delta_2) \end{aligned}\right\} \quad \text{as} \quad z \to \mathrm{i}\delta_2. \tag{2.8}$$

Suppose that the interface between the two fluid layers is some curve $\eta(x)$. The unknown angle of entry α into the sink is then found from

$$\eta'(0) = \tan \alpha. \tag{2.9}$$

Far upstream the interface becomes horizontal, so that

$$\lambda_2 = \eta(\infty). \tag{2.10}$$

The fact that neither of the two fluids is free to cross this interface gives rise to two kinematic conditions

$$v_j = u_j \frac{\mathrm{d}\eta}{\mathrm{d}x}, \quad j = 1, 2, \tag{2.11}$$

to be satisfied on the interface $\eta(x)$. There is also a dynamic boundary condition at the interface, which expresses the fact that the pressure must be continuous on crossing this free boundary, from one fluid to the other. An expression for the pressure in each layer may be obtained simply from the Bernoulli equation, and equating the two pressures at the interface gives the condition

$$\tfrac{1}{2}DF_T^2\left(u_1^2+v_1^2\right)-\tfrac{1}{2}F_T^2\left(u_2^2+v_2^2\right)+(D-1)\eta=\tfrac{1}{2}DF_1^2\lambda_1-\tfrac{1}{2}F_2^2\lambda_2+(D-1)\lambda_2 \quad (2.12)$$

which holds along the curve $\eta(x)$.

Since the interface $\eta(x)$ passes right into the sink, at which point the velocities in each fluid layer are singular, special attention must be given to the Bernoulli equation there. We follow Hocking (1995) by observing that, when the relations (2.8) are substituted into the interface condition (2.12), a solution is only possible if the singular part is removed. This requires us to take

$$\tfrac{1}{2}DF_T^2\left(\frac{2\theta_1}{\pi-2\alpha}\right)^2=\tfrac{1}{2}F_T^2\left(\frac{2\theta_2}{\pi+2\alpha}\right)^2,$$

from which another relationship between the dimensionless parameters may be derived in the form

$$\theta_2=\frac{(\pi+2\alpha)D^{1/2}}{(\pi+2\alpha)D^{1/2}+(\pi-2\alpha)}. \quad (2.13)$$

The governing equations (2.5) within each fluid and the duct boundary conditions (2.7) are satisfied identically, by making use of an integral equation in each of the two layers. This procedure has become rather standard for problems of this type, and so it is only necessary to give a brief overview of the derivation here. The equivalent procedure for the case in which both fluids are of infinite depth is outlined by Hocking (1995).

The complex potential f_2 in the lower fluid becomes singular at the extraction point $z=\mathrm{i}\delta_2$ in the manner defined by equation (2.8), and this behaviour must also be incorporated into the integral equation. In addition, the boundary condition (2.7) at the lower wall $y=0$ must be satisfied by the method of images, reflecting the lower fluid 2 about the line $y=0$, to form an image system with an image interface at $y=-\eta(x)$. For this reason, it is necessary to consider the complex function

$$\chi_2(z)=\frac{\mathrm{d}f_2}{\mathrm{d}z}+\frac{2\theta_2}{(\pi+2\alpha)}\left[\frac{1}{z-\mathrm{i}\delta_2}+\frac{1}{z+\mathrm{i}\delta_2}\right],$$

which is analytic in the lower fluid 2 and its image in the line $y=0$, and which accounts for the singular behaviour of the velocity $\mathrm{d}f_2/\mathrm{d}z$ at the sink point $z=\mathrm{i}\delta_2$ and its image at $z=-\mathrm{i}\delta_2$. It is convenient to write the real and imaginary parts of this function explicitly, so that

$$\chi_2(x,y)=A_2(x,y)-\mathrm{i}B_2(x,y), \quad (2.14a)$$

with

$$\left.\begin{aligned}A_2(x,y)&=u_2(x,y)+\frac{2\theta_2}{(\pi+2\alpha)}\left[\frac{x}{x^2+(y-\delta_2)^2}+\frac{x}{x^2+(y+\delta_2)^2}\right],\\ B_2(x,y)&=v_2(x,y)+\frac{2\theta_2}{(\pi+2\alpha)}\left[\frac{(y-\delta_2)}{x^2+(y-\delta_2)^2}+\frac{(y+\delta_2)}{x^2+(y+\delta_2)^2}\right].\end{aligned}\right\} \quad (2.14b)$$

Here, u_2 and v_2 are the components of the velocity vector in the lower fluid 2, as before.

Cauchy's integral formula

$$\oint \frac{\chi_2(z_P)\,\mathrm{d}z_P}{z_P - z_Q} = 0 \tag{2.15}$$

is applied to the analytic function $\chi_2(z)$ in equation (2.14*a*), on a path consisting of the entire interfacial free surface and its image below the line $y = 0$, connected by vertical line segments infinitely far upstream. Additionally, the fixed point z_Q on the interface is bypassed with a semicircular contour of vanishingly small radius. In order to satisfy the bottom boundary condition (2.7) identically (on the surface $y = 0$), the reflection conditions

$$A_2(x,-y) = A_2(x,y), \quad B_2(x,-y) = -B_2(x,y) \tag{2.16}$$

are imposed, and these equations allow variables at the image free surface to be expressed in terms of quantities at the true interface $\eta(x)$. The flow is also left-right symmetric, and this is expressed by the relations

$$A_2(-x,y) = -A_2(x,y), \quad B_2(-x,y) = B_2(x,y). \tag{2.17}$$

When the conditions (2.16) and (2.17) are incorporated into the Cauchy formula (2.15), after some algebra there results the integral equation

$$\begin{aligned}
\pi A_2(Q) = &-\int_0^\infty \frac{\left[\Delta\eta^- A_2(P) + \Delta x^+ B_2(P)\right] - \eta'(P)\left[\Delta x^+ A_2(P) - \Delta\eta^- B_2(P)\right]}{\left(\Delta x^+\right)^2 + \left(\Delta\eta^-\right)^2}\,\mathrm{d}x_P \\
&+\mathrm{CPV}\int_0^\infty \frac{\left[\Delta\eta^- A_2(P) + \Delta x^- B_2(P)\right] - \eta'(P)\left[\Delta x^- A_2(P) - \Delta\eta^- B_2(P)\right]}{\left(\Delta x^-\right)^2 + \left(\Delta\eta^-\right)^2}\,\mathrm{d}x_P \\
&-\int_0^\infty \frac{\left[\Delta\eta^+ A_2(P) + \Delta x^+ B_2(P)\right] - \eta'(P)\left[\Delta x^+ A_2(P) - \Delta\eta^+ B_2(P)\right]}{\left(\Delta x^+\right)^2 + \left(\Delta\eta^+\right)^2}\,\mathrm{d}x_P \\
&+\int_0^\infty \frac{\left[\Delta\eta^+ A_2(P) + \Delta x^- B_2(P)\right] - \eta'(P)\left[\Delta x^- A_2(P) - \Delta\eta^+ B_2(P)\right]}{\left(\Delta x^-\right)^2 + \left(\Delta\eta^+\right)^2}\,\mathrm{d}x_P,
\end{aligned} \tag{2.18}$$

which is valid for flow variables in the lower fluid 2. The prefix CPV before the second integral in equation (2.18) indicates that this is to be interpreted in the Cauchy principal value sense, and for convenience we have defined

$$\Delta x^\pm = x_P \pm x_Q \quad \text{and} \quad \Delta\eta^\pm = \eta(x_P) \pm \eta(x_Q). \tag{2.19}$$

A similar procedure is employed to derive an integral equation for flow variables in the upper fluid layer 1. Since reflection about the upper boundary $y = 1$ is to be used, we apply Cauchy's integral formula to the analytic function

$$\chi_1(z) = \frac{\mathrm{d}f_1}{\mathrm{d}z} + \frac{2\theta_1}{(\pi - 2\alpha)}\left[\frac{1}{z - \mathrm{i}\delta_2} + \frac{1}{z - \mathrm{i}(2 - \delta_2)}\right],$$

on a path consisting of the interface and its image in the line $y = 1$ connected by vertical line segments at infinity, and the point z_Q on the true interface bypassed by a small semicircular arc. As before, the real and imaginary parts of this analytic function are written explicitly as

$$\chi_1(x,y) = A_1(x,y) - \mathrm{i}B_1(x,y),$$

and the reflection condition

$$\chi_1(x,2-y) = A_1(x,y) + \mathrm{i}B_1(x,y)$$

is used, analogously with equations (2.16) in the lower fluid, to satisfy the boundary condition (2.7) identically on the surface $y = 1$. The functions A_1 and B_1 obey the same equations (2.17) as their counterparts in the lower fluid, since the flow is symmetric about the y-axis. Eventually, an integral equation for variables in the upper fluid 1 is obtained, and may be written

$$\begin{aligned}\pi A_1(Q) = &\int_0^\infty \frac{\left[\Delta\eta^- A_1(P) + \Delta x^+ B_1(P)\right] - \eta'(P)\left[\Delta x^+ A_1(P) - \Delta\eta^- B_1(P)\right]}{\left(\Delta x^+\right)^2 + \left(\Delta\eta^-\right)^2}\,\mathrm{d}x_P \\ &-\mathrm{CPV}\int_0^\infty \frac{\left[\Delta\eta^- A_1(P) + \Delta x^- B_1(P)\right] - \eta'(P)\left[\Delta x^- A_1(P) - \Delta\eta^- B_1(P)\right]}{\left(\Delta x^-\right)^2 + \left(\Delta\eta^-\right)^2}\,\mathrm{d}x_P \\ &+\int_0^\infty \frac{\left[(\Delta\eta^+ - 2)A_1(P) + \Delta x^+ B_1(P)\right] - \eta'(P)\left[\Delta x^+ A_1(P) - (\Delta\eta^+ - 2)B_1(P)\right]}{\left(\Delta x^+\right)^2 + \left(\Delta\eta^+ - 2\right)^2}\,\mathrm{d}x_P \\ &-\int_0^\infty \frac{\left[(\Delta\eta^+ - 2)A_1(P) + \Delta x^- B_1(P)\right] - \eta'(P)\left[\Delta x^- A_1(P) - (\Delta\eta^+ - 2)B_1(P)\right]}{\left(\Delta x^-\right)^2 + \left(\Delta\eta^+ - 2\right)^2}\,\mathrm{d}x_P.\end{aligned} \tag{2.20}$$

The task is now to solve the interfacial conditions (2.9)–(2.12) together with the two integral equations (2.18) and (2.20), subject to the requirements (2.6) and (2.13) and the various relationships (2.2)–(2.4) among the physical parameters. This is done in a straightforward manner using Newton's method, and is outlined briefly in the next section.

3. The numerical solution

A numerical solution is sought, on a grid of evenly spaced points $x_1, x_2, \ldots, x_N$ along the x-axis, for which the uniform mesh spacing is h. Here, $x_1 = 0$ and x_N should be chosen to be as large as possible. The unknown interface location $\eta(x)$ is approximated by the set of discrete values $\eta_1, \eta_2, \ldots, \eta_N$ and the surface slope is represented as $\eta'_1, \eta'_2, \ldots, \eta'_N$. The velocity components $u_2(x)$ and $v_2(x)$ at the interface, in lower layer 2, are approximated by point values $u_j^{(2)}$ and $v_j^{(2)}$, for $j = 1, 2, \ldots, N$, and in the upper fluid layer 1, the velocity components are approximately $u_j^{(1)}$ and $v_j^{(1)}$, $j = 1, 2, \ldots, N$.

The four parameters δ_2 the sink elevation, D the density ratio, λ_2 the upstream interface height and F_T the total withdrawal Froude number are first specified, and a guess is then made for the vector of unknowns

$$\boldsymbol{U} = [\alpha; \eta'_2, \ldots, \eta'_{N-1}; u_2^{(1)}, \ldots, u_N^{(1)}; u_2^{(2)}, \ldots, u_N^{(2)}]^T. \tag{3.1}$$

Equation (2.9) immediately gives the surface slope η'_1 at the first point $x_1 = 0$, and since the interface is drawn into the sink, the condition $\eta_1 = \delta_2$ is also imposed. Far upstream the flow is uniform, and we specify $\eta'_N = 0$ there. The withdrawal fraction θ_2 in the lower layer is obtained from equation (2.13), and the remaining parameters λ_1, θ_1 and the two Froude numbers F_1 and F_2 are found using equations (2.2) and (2.3).

The remaining flow variables are now constructed from this initial guess (3.1). Simple trapezoidal rule integration allows the interface $\eta(x)$ to be estimated, according

to the recursive formula

$$\eta_{j+1} = \eta_j + \frac{h}{2}\left[\eta'_j + \eta'_{j+1}\right], \quad j = 1, 2, \ldots, N-1.$$

The vertical components of velocity in each layer are estimated at every mesh point, except the first, by means of the kinematic boundary conditions (2.11), which in their discrete approximations become

$$v_j^{(1)} = u_j^{(1)}\eta'_j, \quad v_j^{(2)} = u_j^{(2)}\eta'_j, \quad j = 2, 3, \ldots, N.$$

The initial guess (3.1) is updated iteratively, using Newton's method to force the residual error vector

$$\boldsymbol{E}(\boldsymbol{U}) = [E_1, \ldots, E_{N-1}; E_N, \ldots, E_{2N-2}; E_{2N-1}, \ldots, E_{3N-3}]^T \tag{3.2}$$

to zero. The first $N-2$ elements of this vector $E_1, \ldots, E_{N-2}$ are obtained from the Bernoulli equation (2.12) evaluated at the points $x_2, \ldots, x_{N-1}$. The condition (2.10) is imposed by requiring that

$$E_{N-1} = \eta_N - \lambda_2.$$

The next $N-1$ elements $E_N, \ldots, E_{2N-2}$ come from evaluating the integral equation (2.20) in upper fluid 1 at the half-mesh points $x_{j+1/2}$, $j = 1, \ldots, N-1$. Since the Cauchy principal value singularity is now located half way between mesh points, it can be ignored in the integration, by symmetry, so that no special techniques are needed to cope with it. The sink conditions (2.8) show that special treatment is required at the first mesh point $x_1 = 0$, however, since the interface is drawn right into the sink at this point. It may be shown that these conditions are equivalent to taking

$$A_1 \to 0, \quad B_1 \to \frac{\theta_1}{(\pi - 2\alpha)(\delta_2 - 1)} \quad \text{as} \quad x \to 0,$$

and these are easily incorporated into the numerical evaluation of the integrals in equation (2.20). It is also necessary to estimate the portion of each integral in (2.20) that is lost in the truncation process; that is, an approximate formula is required for the steady flow region in the interval $x_N < x < \infty$. Here, it is sufficient to take $\eta \approx \lambda_2$, $\eta' \approx 0$, and velocity components given approximately by equations (2.6). The tails of the integrals ignored in the truncation may then be estimated in closed form. The final $N-1$ error elements $E_{2N-1}, \ldots, E_{3N-3}$ in the residual vector (3.2) are likewise obtained by evaluating the integral equation (2.18) at the $N-1$ half-mesh points as before, making use of the relations

$$A_2 \to 0, \quad B_2 \to \frac{\theta_2}{(\pi + 2\alpha)\delta_2} \quad \text{as} \quad x \to 0$$

at the first mesh point $x_1 = 0$, and estimating the tails of the integrals beyond the truncation point $x = x_N$, as before.

A (damped) Newton's method solution of these equations, $\boldsymbol{E} = \boldsymbol{0}$, generally converges rapidly from a suitable initial guess, and several choices for this starting guess are given in the next section. Once a solution has been found to the full system of equations, it can be used as a starting point for other solutions, and in this way, an entire solution branch can be tracked.

4. Closed-form solutions in special cases

In this section, we present two solutions to the governing equations, in two special situations in which exact closed-form solutions are possible. In some sense these are trivial situations, but the solutions thus obtained are nevertheless useful, both as starting points for the Newton's method algorithm of §3, and as points of reference against which to check the accuracy of the numerical method itself.

4.1. *Exact solution for* $\lambda_2 = \delta_2 = 1/2$

When the sink elevation $\delta_2 = 1/2$, then there is an exact solution for which the interface is simply a flat surface. In this case therefore,

$$\eta(x) = \lambda_2 = \delta_2 = 1/2. \tag{4.1}$$

It follows at once that the entry angle α of the interface into the sink is simply $\alpha = 0$, and then from equations (2.13) and (2.2) the withdrawal fractions in each fluid layer become

$$\theta_1 = \frac{1}{1 + D^{1/2}} \quad \text{and} \quad \theta_2 = \frac{D^{1/2}}{1 + D^{1/2}}. \tag{4.2}$$

The complex potentials f_1 and f_2 in the two fluid layers are therefore found as the solution to a problem in which the interface is the horizontal line $\eta = 1/2$, with a line sink on this interface at $x = 0$. This problem can be solved by conformal mapping. These potentials are calculated to be

$$\left.\begin{aligned} f_1(z) &= -\frac{\theta_1}{\pi}\ln(\tfrac{1}{4}[\cosh(2\pi(z - \mathrm{i}\tfrac{1}{2})) - 1]), \\ f_2(z) &= -\frac{\theta_2}{\pi}\ln(\tfrac{1}{4}[\cosh(2\pi z) + 1]), \end{aligned}\right\} \tag{4.3}$$

and so, along the interface (4.1), the fluid velocities in each layer are

$$\left.\begin{aligned} u_1 - \mathrm{i}v_1 &= \frac{\mathrm{d}f_1}{\mathrm{d}z} = -2\theta_1 \coth[\pi x] \\ u_2 - \mathrm{i}v_2 &= \frac{\mathrm{d}f_2}{\mathrm{d}z} = -2\theta_2 \coth[\pi x] \end{aligned}\right\} \quad \text{on} \quad \eta = \delta_2 = 1/2. \tag{4.4}$$

4.2. *Solution for* $D = 1$

In the case when the density ratio D is exactly 1, the two-fluid system becomes merely a single fluid in a duct, and the interface disappears. Any streamline in the flow is then a potential interface, and the particular streamline chosen would depend on the value of the upstream depth λ_2.

For flow in a duct of height 1, produced by a line sink at the location $z = \mathrm{i}\delta_2$, conformal mapping at once yields the solution

$$f(z) = -\frac{1}{\pi}\ln\left[\tfrac{1}{2}\cosh(\pi z) - \tfrac{1}{2}\cos(\pi\delta_2)\right], \tag{4.5}$$

where now $f_1 = f_2 = f$. Solutions of this type may be found in the book by Milne-Thomson (1979), for example.

Suppose that a particular streamline $-1 \leqslant \psi \leqslant 0$ is chosen. After some algebra, equation (4.5) may be inverted to give the shape of this streamline in the form

$$y(x;\psi) = \frac{1}{\pi}\arccos\left[\frac{B + (B^2 - AC)^{1/2}}{A}\right], \tag{4.6a}$$

in which, for convenience, we have defined the intermediate functions

$$\left.\begin{aligned} A &= \sin^2(\pi\psi)\cosh^2(\pi x) + \cos^2(\pi\psi)\sinh^2(\pi x), \\ B &= \sin^2(\pi\psi)\cos(\pi\delta_2)\cosh(\pi x), \\ C &= \sin^2(\pi\psi)\cos^2(\pi\delta_2) - \cos^2(\pi\psi)\sinh^2(\pi x). \end{aligned}\right\} \tag{4.6b}$$

Careful perturbation analysis of this streamline shape (4.6) near $x = 0$ shows that the entry angle for this streamline is

$$\alpha = \pi\psi + \frac{\pi}{2}, \quad -1 \geqslant \psi \geqslant 0, \tag{4.7}$$

as is to be expected on physical grounds. As in §4.1, the fluid velocities along this streamline can now be computed by (complex) differentiation of equation (4.5).

Equations (4.6) and (4.7) take a particularly simple form for the streamline $\psi = -1/2$. The streamline shape (4.6) becomes simply

$$\eta(x) = \frac{1}{\pi}\arccos\left(\frac{\cos(\pi\delta_2)}{\cosh(\pi x)}\right) \quad \text{on} \quad \psi = -1/2, \tag{4.8}$$

and the entry angle of the interface into the sink is simply $\alpha = 0$ for $\psi = -1/2$, which follows from equation (4.7). Along the streamline (4.8), the fluid velocities are

$$u = -\coth(\pi x), \quad v = -\frac{\cos(\pi\delta_2)}{[\cosh^2(\pi x) - \cos^2(\pi\delta_2)]^{1/2}} \quad \text{on} \quad \psi = -1/2. \tag{4.9}$$

These formulae (4.6)–(4.9) provide useful starting solutions for the Newton method algorithm in §3.

5. Presentation of results

The numerical method of §3 has been run extensively to construct a reasonably comprehensive description of the behaviour of solutions to the fully nonlinear model outlined in §2. Nearly 1000 separate numerical solutions have been obtained over a wide variety of parameter values. The numerical scheme has usually been run with $N = 151$ mesh points placed on the interface (only half of which needs be considered, by symmetry, as outlined in §2), and this requires the use of Newton's method in 450 variables. As a check on the numerical accuracy of these solutions, we have compared them to results obtained with $N = 301$ interfacial surface points for selected parameter values. (This involves a Newton's method solution with 900 variables, which is a significant numerical undertaking.) It has been determined that the solutions obtained here are insensitive, to graphical accuracy, to the number of mesh points and the numerical window $x_1 < x < x_N$ over which the points are placed.

5.1. *High D and moderate F_T*

It is to be expected that the two fluids within the duct would normally be of very similar densities, so that the dimensionless density ratio D would be expected to be close to 1, on physical grounds. For this reason, we begin this section with an investigation of the case $D = 0.95$, and with a total Froude number $F_T = 0.5$.

Figure 2 shows how the entry angle α of the interface into the sink varies with the depth λ_2 of the interface far upstream. Results are given for three different values of the sink elevation $\delta_2 = 0.25$, 0.5 and 0.75. In each case, the results are as would

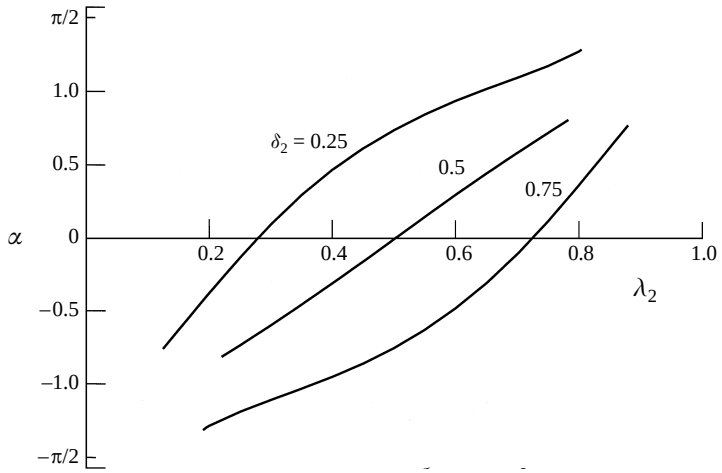

FIGURE 2. The variation of the entry angle α with the upstream interface height λ_2, for the case $D = 0.95$, $F_T = 0.5$. Three sets of results are shown, for sink elevations $\delta_2 = 0.25$, 0.5 and 0.75.

be expected intuitively. For small λ_2, the lower fluid 2 is very shallow, and must rise steeply to enter the sink, at the point $(x, y) = (0, \delta_2)$; therefore, the entry angle α is close to the value $\alpha = -\pi/2$ at which entry is exactly vertical. As the upstream depth λ_2 is increased, the entry angle α increases, and for sufficiently large λ_2 the results suggest that the interface ultimately drops vertically into the sink, with entry angle $\alpha = \pi/2$.

Our numerical scheme does not permit us to compute solutions right up to the limiting configurations at which entry into the sink is vertical, with $\alpha = \pm\pi/2$. This is scarcely surprising, but there seems no reason to doubt that the limiting configurations do indeed involve vertical entry of the interface into the sink, and that, with sufficiently many numerical mesh points and perhaps with the use of arclength as the independent variable along the interface and a non-uniform mesh, results should be possible with interface sections arbitrarily close to the vertical. Hocking (1995), in his study of simultaneous withdrawal of two fluids of infinite depth, paid very close attention to the (single) limiting configuration in his problem, at which the interface was drawn down vertically with $\alpha = \pi/2$, and presented strong numerical evidence that this limiting solution was related to the isolated solution found by Tuck & Vanden-Broeck (1984), at which a cusp formed directly above the line sink, but only exists at one value of the withdrawal Froude number. This is an important result, as it shows that the withdrawal Froude number found by Tuck & Vanden-Broeck really is the point at which the interface collapses into the sink, and the upper fluid is also withdrawn; such a result has practical significance for reservoir management, for example. Nevertheless, Hocking's numerical scheme likewise could not continue for values of the entry angle α greater than about 1.3, and he used extrapolative curve fitting to show that, at the limiting entry angle $\alpha = \pi/2$, he recovered the Froude number of Tuck & Vanden-Broeck as a limiting case. In the present problem, we have similarly managed to compute solutions in the approximate interval $0 \leqslant |\alpha| \leqslant 1.3$.

These limiting configurations in figure 2, at which the interface near the sink becomes vertical with entry angles $\alpha = -\pi/2$ and $\alpha = \pi/2$, would correspond to withdrawal fractions $\theta_2 = 0$ and $\theta_2 = 1$, respectively. These situations represent withdrawal totally from only one of the fluid layers, i.e. selective withdrawal. It can

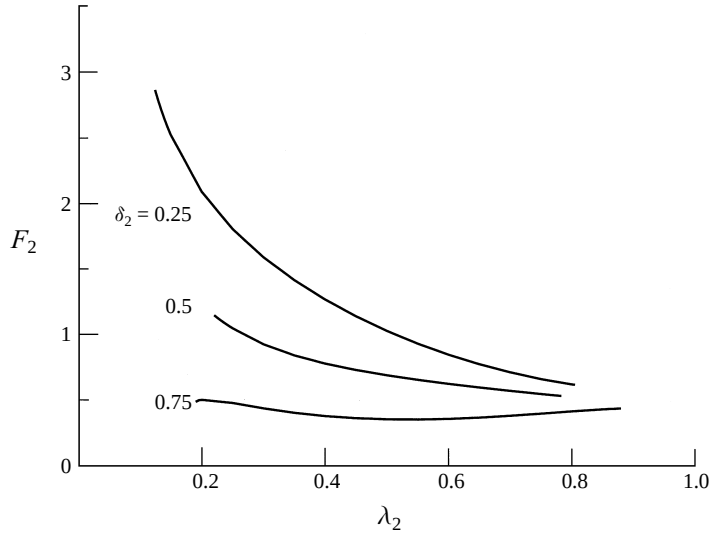

FIGURE 3. The variation of the Froude number F_2 in the lower layer with the upstream interface height λ_2, for the case $D = 0.95$, $F_T = 0.5$. Three sets of results are shown, for sink elevations $\delta_2 = 0.25$, 0.5 and 0.75.

be demonstrated by an exact analysis of the governing equations that the curves for sink height $\delta_2 = 0.25$ and $\delta_2 = 0.75$ in figure 2 must be antisymmetrical, and this is confirmed by the numerical results. This serves as a useful additional check on the accuracy of the numerical scheme. It will be shown later that the present solutions are supercritical with respect to the appropriate combination Froude number.

Figure 3 shows the way in which the Froude number F_2 in the lower fluid layer varies with upstream depth λ_2 for the case $D = 0.95$ and $F_T = 0.5$, and for the three sink elevations $\delta_2 = 0.25$, 0.5, and 0.75, as in figure 2. The Froude number F_2 is a derived quantity and can be eliminated in favour of the principal parameters in the problem, as shown by equations (2.3), and so is not strictly necessary in the formulation of this problem. Nevertheless, it gives an indication of flow conditions in the lower layer. Thus, for sink elevation $\delta_2 = 0.75$, conditions in the lower layer evidently do not change greatly with changes to the upstream depth λ_2, as reflected by the fact that the Froude number F_2 in this layer remains roughly constant, so that decreases in upstream depth λ_2 are matched by a compensating drop in withdrawal fraction θ_2. By contrast, the curve obtained with sink height $\delta_2 = 0.25$ shows a strong increase in the Froude number F_2 with decreasing depth λ_2. Thus for $\delta_2 = 0.25$, lower layer 2 becomes a fast flowing shallow layer as λ_2 is decreased. By invoking symmetry, as discussed in relation to figure 2, the results for F_1 can be obtained by replacing λ_2 with λ_1, F_2 with F_1 and interchanging the values of δ_2 in figure 3.

Three interface profiles are displayed in figure 4 for this case in which the density ratio is $D = 0.95$ and the total Froude number is $F_T = 0.5$. In this diagram, the upstream depth has been fixed at the value $\lambda_2 = 0.5$, and the three solutions correspond to sink elevations $\delta_2 = 0.25$, 0.5 and 0.75. The dashed line is the interface profile for the case $\delta_2 = \lambda_2 = 0.5$, which by the result of §4.1, is simply the horizontal surface $\eta(x) = 0.5$.

The interface profiles in figure 4 were obtained with $N = 301$ points distributed over the interval $0 \leqslant x \leqslant 18$ (and the full interface was obtained by reflection about the y-axis). The portions of the interfaces at least in the interval $-5 < x < 5$ in

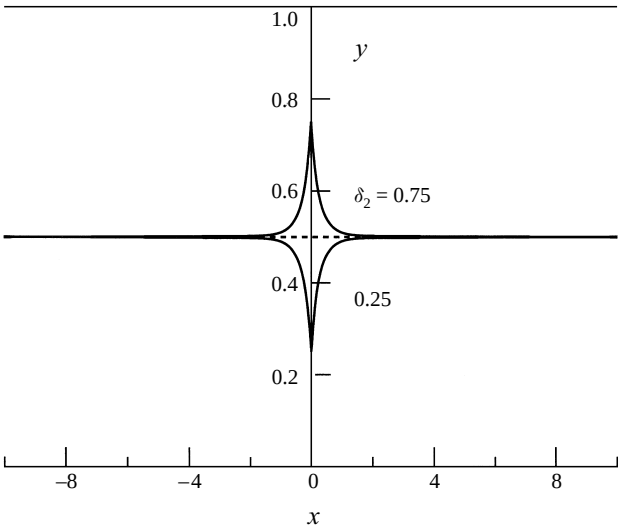

FIGURE 4. Three interface profiles for $D = 0.95$, $F_T = 0.5$, $\lambda_2 = 0.5$, at the three different values of the sink elevation $\delta_2 = 0.25$, 0.5 and 0.75.

figure 4 have been demonstrated to be insensitive to the details of the numerical discretization process, at least to graphical accuracy, and so may be considered to be accurate converged solutions. Again, the symmetry of the two interface profiles for $\delta_2 = 0.25$ and 0.75 is confirmed.

5.2. *Exploration of mathematical solution branches*

In §5.1, solutions were presented for cases in which the density ratio D was very close to 1, and the Froude number F_T was of moderate size. We now consider what becomes of the solution branch shown in figures 2–4 when these conditions do not hold.

In figure 5, solutions have been computed for sink elevation $\delta_2 = 0.25$ and density ratio $D = 0.95$, over a range of different total Froude number F_T values. For F_T larger than about 0.2, the interface profile and entry angle α are reasonably insensitive to the choice of Froude number F_T, and the angle is maintained at about $\alpha = 0.75$ over much of figure 5 (solutions for F_T larger than 1 have also been obtained, but are not shown here). However, as F_T is decreased, a sufficiently small value is reached, beyond which the entry angle α drops very rapidly. Indeed, the change of α with F_T becomes so rapid that issues of numerical accuracy prevent us from following the entire solution branch, but it seems highly likely that a finite (small) Froude number will be achieved for which the entry angle becomes vertical, with $\alpha = -\pi/2$. This is evidently the limiting interfacial profile formed at some minimum Froude number.

An initially unexpected feature of the results shown in figure 5 is that the portion on the extreme left of the diagram, for which the angle α changes very rapidly, is actually a different mathematical branch of solutions from those obtained with larger Froude number. The gap in the curve in figure 5 is a portion for which numerical solutions could not be obtained, and it appears that some sort of resonance between the two solution branches occurs in this narrow interval (approximately $0.10 < F_T < 0.11$). To the right of this gap, for $F_T \gtrsim 0.11$, the solution branch is uniquely defined by the four parameters δ_2, D, F_T and λ_2 ($= 0.5$ here), and these four parameters may be specified in advance, as for the solutions shown in figures 2–4. However, the branch

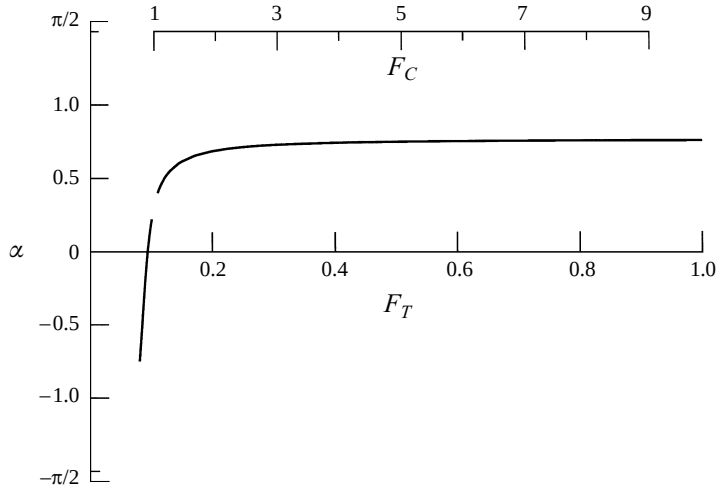

FIGURE 5. The variation of the entry angle α with the withdrawal Froude number F_T, for the case $\delta_2 = 0.25$, $D = 0.95$. Solutions to the right of this figure have been obtained with $\lambda_2 = 0.5$. The combination Froude number F_C is also indicated.

of solutions to the left of the gap, for $F_T \lesssim 0.10$, have the property that the upstream depth λ_2 is not free to be specified in advance if the other three parameters are already fixed, but is instead obtained as part of the solution. This has been confirmed by altering the numerical method in §3 so as to allow the Bernoulli equation (2.12) to be satisfied at the mesh points $x_2, \ldots, x_N$ and then estimating the upstream depth λ_2 from the converged solution for η_N, thus imposing condition (2.10) explicitly in the numerical method. (In fact, the change of angle α with Froude number F_T for this branch of solutions is so rapid that we generally specify α in advance, and have the numerical method solve for both F_T and λ_2.)

These two different solution branches in figure 5 can be explained by reference to the combination Froude number for the two-fluid system, obtained from hydraulic theory. We show in the Appendix that the appropriate combination Froude number F_C for this two-fluid system is obtained from the formula

$$F_C^2 = \frac{F_2^2 + DF_1^2}{1 - D}, \tag{5.1}$$

where F_1 and F_2 are the two local Froude numbers in layers 1 and 2, as defined in equations (2.3). (Results of this type for two-fluid systems are given in Armi 1986 and Forbes 1989.) This combination Froude number is easily computed from our numerical solutions, and its values are indicated by the axis at the top of figure 5.

It can be seen that the resonance near $F_T = 0.11$ occurs precisely at the critical value $F_C = 1$. Thus the branch of solutions to the right of this gap near $F_T = 0.11$ corresponds to supercritical solutions, and represents an extension of the results computed by Hocking (1995) for two-fluid systems of infinite depth. By contrast, the isolated branch to the left of figure 5 (for which the depth λ_2 is not free to be specified) is a subcritical solution branch.

A representative solution from each of the two branches in figure 5 is displayed in figure 6. The upper profile, for Froude number $F_T = 0.5$, is one for which the upstream interface height $\lambda_2 = 0.5$ has been specified in advance; in fact, this solution has already been presented in figure 4 (for $\delta_2 = 0.25$), and represents a

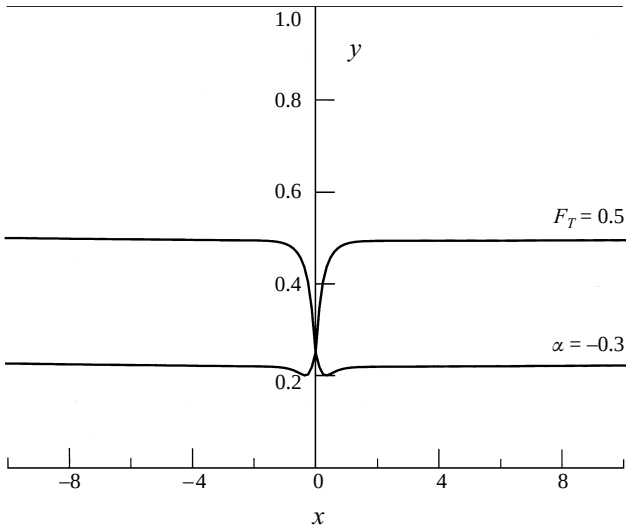

FIGURE 6. Two interface profiles for $\delta_2 = 0.25$, $D = 0.95$. The top solution has been obtained with $F_T = 0.5$ and $\lambda_2 = 0.5$. In the bottom solution, the entry angle was set to the value $\alpha = -0.3$, and both the Froude number and the upstream depth were determined from the numerical solution.

supercritical solution, with combination Froude number $F_C \approx 4.9$. By contrast, the solution obtained with $\alpha = -0.3$ (for which $F_T \approx 0.089$) has selected its own upstream interface height $\lambda_2 \approx 0.22$, and is a subcritical solution.

Figures 5 and 6 therefore show that, for moderate and large Froude numbers, there is a continuum of supercritical solutions for fixed values of the sink elevation δ_2, the density ratio D and the Froude number F_T, since the upstream interface height λ_2 may be chosen arbitrarily. However, for each small Froude number F_T, an isolated subcritical solution exists for a unique interface height λ_2. This result has some similarities to the work of Hocking & Forbes (1992), as is discussed in §6.

The effect of varying the Froude number F_T is again examined in figure 7, this time for a different sink elevation $\delta_2 = 0.75$. The density ratio has again been set at $D = 0.95$. In this diagram, results are presented for two different values of the upstream interface height, $\lambda_2 = 0.25$ and 0.5 in the supercritical ($F_C > 1$) case. There is a continuum of such curves for different values of λ_2, each of which terminates as the critical value of the combination Froude number $F_C = 1$ is approached from above. The dashed line denotes the subcritical solution branch; this is an isolated branch, along which the depth λ_2 cannot be specified in advance, and varies with F_T. The results suggest that there is a limiting profile on the subcritical branch, when the interface drops vertically into the sink with entry angle $\alpha = \pi/2$.

Three different interface profiles are shown for this case $\delta_2 = 0.75$, $D = 0.95$ in figure 8. The lower two profiles have both been obtained with Froude number $F_T = 0.4$ ($F_C > 1$), and upstream depths $\lambda_2 = 0.25$ and 0.5, as indicated on the diagram. These are from the same supercritical branch of solutions discussed above, in which the upstream depth λ_2 is free to be given in advance. The top most interface profile, however, corresponds to $\alpha = 0.5$ in figure 7 (with $F_T \approx 0.084$); it is an example of the subcritical branch of solutions (sketched with a dashed line in figure 7) for which the upstream depth λ_2 cannot be specified in advance, but instead finds its own level.

So far, results have been shown with fixed density ratio $D = 0.95$, since this is likely to represent the situation that would be observed experimentally. For (mathematical)

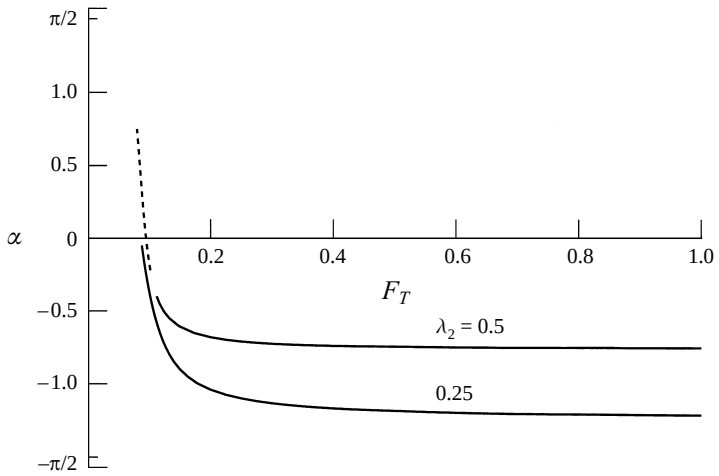

FIGURE 7. The variation of the entry angle α with the withdrawal Froude number F_T, for the case $\delta_2 = 0.75$, $D = 0.95$. Two sets of supercritical results are shown, for upstream interface heights $\lambda_2 = 0.25$ and 0.5. The isolated subcritical branch of solutions (sketched with a dashed line) is a branch of solutions for which λ_2 is determined as part of the solution.

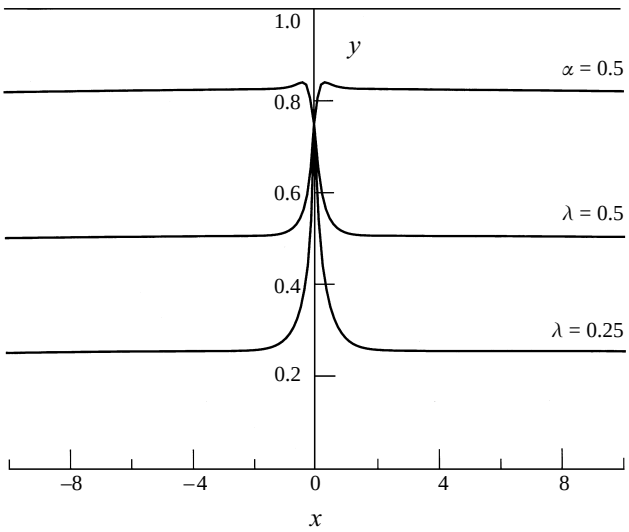

FIGURE 8. Three interface profiles for $\delta_2 = 0.75$, $D = 0.95$. The bottom solution has been obtained with $F_T = 0.4$ and $\lambda_2 = 0.25$, and the middle surface represents $F_T = 0.4$ and $\lambda_2 = 0.5$. In the top solution, the entry angle was set to the value $\alpha = 0.5$, and both the Froude number and the upstream depth were determined from the numerical solution.

completeness, we finish this presentation of the results by investigating the way in which solutions vary with the density ratio D. This is illustrated in figure 9, for the case in which the sink elevation is $\delta_2 = 0.25$ and the Froude number is fixed at the moderate value $F_T = 0.5$. This graph shows features that are completely analogous to those seen in figures 5 and 7; for values of density ratio D close to 1, there is a branch of supercritical solutions for which all four parameters δ_2, F_T, D and λ_2 (= 0.5 here) are free to be specified independently, as in §5.1. However, as D is decreased, a separate subcritical branch of solutions is encountered, for which only three of these

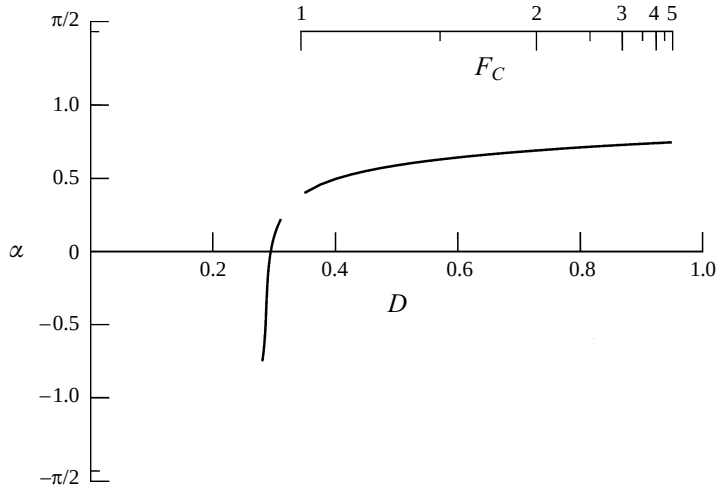

FIGURE 9. The variation of the entry angle α with the density ratio D, for the case $\delta_2 = 0.25$, $F_T = 0.5$. Solutions to the right of this figure have been obtained with $\lambda_2 = 0.5$. The combination Froude number F_C is also indicated.

parameters can be specified in advance and the fourth parameter (λ_2 in this case) is obtained as part of the solution. There is again a narrow interval $0.31 < D < 0.35$ of values of the density ratio for which the numerical method could not yield a steady solution, and it is clear that the combination Froude number F_C takes the critical value $F_C = 1$ within this interval, as shown on the figure. The entry angle α drops very sharply on the subcritical branch to the left of figure 9, and it seems that a limiting value of the density ratio D will be reached, at which the interface rises vertically into the sink, with angle $\alpha = -\pi/2$. Notice that, according to equation (5.1), the combination Froude number F_C becomes infinite as $D \to 1$.

Two interface profiles are shown in figure 10, for the same values of the parameters as in figure 9. The sink is located at the height $\delta_2 = 0.25$, and the upper profile is for $D = 0.95$. The interface far upstream has height $\lambda_2 = 0.5$, and the surface drops sharply into the sink; this is the supercritical solution that would be expected in practice (and has been sketched in figure 4). The lower profile has been obtained with $D = 0.286$, and represents a point on the other subcritical solution branch to the extreme left of figure 9. For this solution, the upstream depth λ_2 cannot be specified in advance, but is computed from the numerical method to be about 0.22.

6. Conclusion and discussion

In this paper, we have examined a class of withdrawal problems for two-layer flow within a confined duct, in which a line sink is present at some point within the fluid system. The interface is drawn into the sink, and both fluids are therefore withdrawn simultaneously. The fluids have been assumed to be flowing uniformly far upstream.

For moderate Froude number and density ratio close to 1, the results are in accordance with physical intuition. There are four parameters which are free to be specified essentially arbitrarily; these are the sink elevation δ_2, the Froude number F_T at which both fluids are withdrawn from the duct, the density ratio D and the upstream depth λ_2 of the interface. For combination Froude number F_C greater than

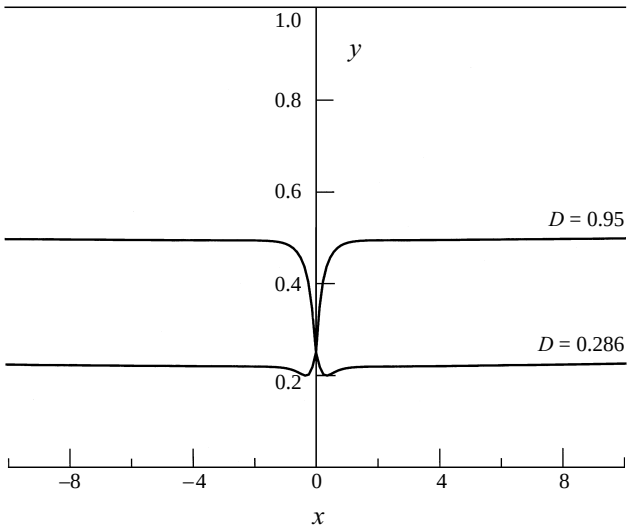

FIGURE 10. Two interface profiles for $\delta_2 = 0.25$, $F_T = 0.5$. The top solution has been obtained with $D = 0.95$ and $\lambda_2 = 0.5$. In the bottom solution, the density ratio is $D = 0.286$, and both the entry angle and the upstream depth were determined from the numerical solution.

1, these four parameters define a unique supercritical solution of the problem, and the angle α at which the interface enters the sink is obtained from this solution.

It is evident from our numerical solutions that there are two possible limiting profiles for flow in a duct. In both cases, the limiting flow involves a vertical entry of the interface into the sink. In one extreme the interface enters the sink from above, with $\alpha = \pi/2$, and in the other limiting case the interface enters vertically from below, with $\alpha = -\pi/2$. These limiting cases are characterized by the fact that they withdraw all their fluid from only one of the fluid layers, and hence can be considered as selective withdrawal solutions.

It is difficult to compare the solutions to the present problem with the solutions obtained by Hocking (1995), since his work involved two fluids both of infinite depth. Thus Hocking's solutions represent a particular type of limit in the present problem, at which the total Froude number $F_T \to 0$. It is evident that the presence of the two walls of the duct at $y = 0$ and $y = 1$ in the problem studied here introduces extra complexities into this problem, the most obvious of which is the fact that there are two limiting profiles here for which the interface enters the sink vertically, as opposed to the single limiting profile with $\alpha = \pi/2$ in Hocking's work. This is a consequence of the presence of the lower wall at $y = 0$.

An initially unexpected feature of the solutions to this problem is the fact that, for combination Froude number F_C less than 1, there is a second (subcritical) branch of solutions for which only three of the defining parameters are free to be specified in advance; the fourth parameter (the upstream depth λ_2 of the interface) is obtained as an output. Essentially this same phenomenon has been obtained by other authors in related withdrawal flow problems. The results are summarized most succinctly in figure 5 of the paper by Hocking & Forbes (1992). For withdrawal flows with a cusp in the free surface directly above the sink, it turns out that a unique cusped solution exists below some critical Froude number, and a continuum of cusped solutions exists above that value of Froude number. This is analogous to the situation encountered here, and it may be the case that the presence of both a supercritical and an isolated

subcritical solution branch is a general feature of withdrawal flows in finite-depth fluid systems.

It is interesting to speculate on the relationship between the steady subcritical branch of solutions obtained here, and the solutions to the full unsteady problem. It may be the case that this isolated solution represents a type of choking flow in which the upstream conditions are determined by the flow into the sink. In that case, a fully time-dependent flow would show a travelling wave moving out from the sink and eventually controlling the upstream flow depth and speed. It would be interesting to explore this fully unsteady flow in future research.

The computations in this paper were performed on a Sun ULTRA 1 machine obtained under Australian Research Council (ARC) grant A69600071, and partial support for the project has been provided by ARC grant A89701734. Collaboration between the investigators has been generously supported by a travel grant from Murdoch University. Discussion of some of this material with Dr Tony Watts, of OPCOM Pty. Ltd. (Toowong, Queensland), is gratefully acknowledged, and comments by all three anonymous referees have proved most useful.

Appendix. Calculation of the combination Froude number

The appropriate combination Froude number for this two-layer system can be obtained using shallow-water (hydraulic) theory. The original dimensional variables will be used in this development, and dimensionless Froude numbers will be defined later, as required.

Suppose that the interfacial elevation is described by the function $y = \eta(x)$. In the upper fluid 1, the continuity equation gives rise to the shallow-water approximation

$$u_1(L-\eta) = c_1(L-H_2), \tag{A 1a}$$

in which H_2 is the interface height far upstream and c_1 is the fluid speed there, in layer 1. The total depth of the duct is $L = H_1 + H_2$. If the pressure at the interface far upstream is denoted p_∞, then the approximate momentum equation in fluid layer 1 is

$$\tfrac{1}{2}u_1^2(x) + \frac{1}{\rho_1}p_s(x) + g\eta(x) = \tfrac{1}{2}c_1^2 + \frac{1}{\rho_1}p_\infty + gH_2. \tag{A 1b}$$

Here, the pressure at the interface is $p_s(x)$, so that $p_s(x) \to p_\infty$ as $x \to \infty$.

Since the aim of this section is to determine critical conditions for the flow, suppose that the bottom of the duct is not flat, but has some shape $y = h(x)$. Then, in the shallow-water approximation, the continuity equation becomes

$$u_2(\eta - h) = c_2H_2 \tag{A 2a}$$

and the momentum equation yields

$$\tfrac{1}{2}u_2^2(x) + \frac{1}{\rho_2}p_s(x) + g\eta(x) = \tfrac{1}{2}c_2^2 + \frac{1}{\rho_2}p_\infty + gH_2. \tag{A 2b}$$

It is convenient at this stage to define local Froude numbers

$$f_1(x) = \frac{u_1}{[g(L-\eta)]^{1/2}} \quad \text{and} \quad f_2(x) = \frac{u_2}{[g(\eta-h)]^{1/2}}, \tag{A 3}$$

and observe that, if $h(x) \to 0$ as $x \to \infty$, then $f_1(x) \to F_1$ and $f_2(x) \to F_2$ far upstream, where F_1 and F_2 are the Froude numbers in each layer, as defined in equations (2.3).

It follows from the continuity equation (A 1*a*) in layer 1 that the local surface elevation and fluid velocity in layer 1 can be written in terms of the local Froude number $f_1(x)$ according to the expressions

$$\eta = L - \left(\frac{c_1^2 H_1^2}{g f_1^2}\right)^{1/3}, \quad u_1 = \left(c_1 H_1 g f_1^2\right)^{1/3}. \tag{A 4a}$$

The continuity equation (A 2*a*) in lower layer 2 similarly leads to the formulae

$$\eta = h + \left(\frac{c_2^2 H_2^2}{g f_2^2}\right)^{1/3}, \quad u_2 = \left(c_2 H_2 g f_2^2\right)^{1/3}. \tag{A 4b}$$

The momentum equations (A 1*b*) and (A 2*b*) in each fluid layer may be combined to eliminate the interfacial surface pressure $p_s(x)$. In conjunction with equations (A 4), these eventually lead to the two equations

$$\lambda_1 \frac{F_1^{2/3}}{f_1^{2/3}} + \lambda_2 \frac{F_2^{2/3}}{f_2^{2/3}} = 1 - \frac{h(x)}{L}, \tag{A 5a}$$

$$\begin{aligned} \tfrac{1}{2}\lambda_2 F_2^{2/3} f_2^{4/3} - \tfrac{1}{2} D \lambda_1 F_1^{2/3} f_1^{4/3} + (1-D)\lambda_2 \frac{F_2^{2/3}}{f_2^{2/3}} \\ = \tfrac{1}{2}\lambda_2 F_2^2 - \tfrac{1}{2} D \lambda_1 F_1^2 + (1-D)\lambda_2 - (1-D)\frac{h(x)}{L} \end{aligned} \tag{A 5b}$$

in dimensionless form. When differentiated with respect to the coordinate x, these two equations give rise to the matrix form

$$\begin{bmatrix} \lambda_1 F_1^{2/3} f_1^{-5/3} & \lambda_2 F_2^{2/3} f_2^{-5/3} \\ D\lambda_1 F_1^{2/3} f_1^{1/3} & \lambda_2 F_2^{2/3} f_2^{-5/3}(1 - D - f_2^2) \end{bmatrix} \begin{bmatrix} \partial f_1/\partial x \\ \partial f_2/\partial x \end{bmatrix} = \frac{3h'(x)}{2L} \begin{bmatrix} 1 \\ 1-D \end{bmatrix}. \tag{A 6}$$

Critical conditions will occur in this flow when $h'(x) = 0$, but with a non-trivial solution to the matrix system (A 6). Under these circumstances, the determinant of the coefficient matrix must be zero, and this gives the requirement

$$f_C^2 = \frac{D f_1^2 + f_2^2}{1 - D} = 1. \tag{A 7}$$

The critical condition (A 7) leads at once to the use of the combination Froude number F_C defined in equation (5.1).

REFERENCES

Armi, L. 1986 The hydraulics of two flowing layers with different densities. *J. Fluid Mech.* **163**, 27–58.

Craya, A. 1949 Theoretical research on the flow of nonhomogeneous fluids. *La Houille Blanche* **4**, 44–55.

Forbes, L. K. 1989 Two-layer critical flow over a semi-circular obstruction. *J. Engng Maths* **23**, 325–342.

Forbes, L. K. & Hocking, G. C. 1990 Flow caused by a point sink in a fluid having a free surface. *J. Austral. Math. Soc.* B **32**, 231–249.

Forbes, L. K. & Hocking, G. C. 1993 Flow induced by a line sink in a quiescent fluid with surface-tension effects. *J. Austral. Math. Soc.* B **34**, 377–391.

Forbes, L. K., Hocking, G. C. & Chandler, G. A. 1996 A note on withdrawal through a point sink in fluid of finite depth. *J. Austral. Math. Soc.* B **37**, 406–416.

Hocking, G. C. 1985 Cusp-like free-surface flows due to a submerged source or sink in the presence of a flat or sloping bottom. *J. Austral. Math. Soc.* B **26**, 470–486.

Hocking, G. C. 1988 Infinite Froude number solutions to the problem of a submerged source or sink. *J. Austral. Math. Soc.* B **29**, 401–409.

Hocking, G. C. 1991 Withdrawal from two-layer fluid through line sink. *J. Hydraul. Engng ASCE* **117**, 595–613.

Hocking, G. C. 1995 Supercritical withdrawal from a two-layer fluid through a line sink. *J. Fluid Mech.* **297**, 37–47.

Hocking, G. C. & Forbes, L. K. 1991 A note on the flow induced by a line sink beneath a free surface. *J. Austral. Math. Soc.* B **32**, 251–260.

Hocking, G. C. & Forbes, L. K. 1992 Subcritical free-surface flow caused by a line source in a fluid of finite depth. *J. Engng Maths* **26**, 455–466.

Lister, J. R. 1989 Selective withdrawal from a viscous two-layer system. *J. Fluid Mech.* **198**, 231–254.

Mekias, H. & Vanden-Broeck, J.-M. 1989 Supercritical free-surface flow with a stagnation point due to a submerged source. *Phys. Fluids* A **1**, 1694–1697.

Mekias, H. & Vanden-Broeck, J.-M. 1991 Subcritical flow with a stagnation point due to a source beneath a free surface. *Phys. Fluids* A **3**, 2652–2658.

Milne-Thomson, L. M. 1979 *Theoretical Hydrodynamics*, 5th edn. Macmillan.

Peregrine, D. H. 1972 A line source beneath a free surface. *Math. Research Centre, Univ. Wisconsin Rep.* 1248.

Sautreaux, C. 1901 Mouvement d'un liquide parfait soumis à la pesanteur. Détermination des lignes de courant. *J. Math. Pures Appl.* **7**, 125–159.

Stoker, J. J. 1957 *Water Waves.* Wiley Interscience.

Tuck, E. O. & Vanden-Broeck, J.-M. 1984 A cusp-like free-surface flow due to a submerged source or sink. *J. Austral. Math. Soc.* B **25**, 443–450.

Vanden-Broeck, J.-M. & Keller, J. B. 1987 Free surface flow due to a sink. *J. Fluid Mech.* **175**, 109–117.

Wood, I. R. & Lai, K. K. 1972 Selective withdrawal from a two-layer fluid. *J. Hydraul. Res.* **10**, 475–496.